

A Rayleigh model of cesium fractionation in granite-pegmatite systems

DAVID LONDON^{1,*}

¹Department of Earth Sciences, The University of Memphis, 109 Johnson Hall, Memphis, Tennessee 38152, U.S.A.

ABSTRACT

The K/Cs ratios of K-feldspars from granitic pegmatites are compared to models derived from the Rayleigh equation. The K/Cs and K/Rb ratios of K-feldspars and micas exhibit decreasing values when plotted against their Cs or Rb contents across cogenetic suites of granites and pegmatites and from margin to core of individual bodies. The trends in elemental ratios conform to Rayleigh fractionation for the crystallization of feldspars and micas from a silicate melt. Within two individual pegmatite bodies, the K/Cs ratio of K-feldspar initially falls more rapidly than the Rayleigh model predicts. That might reflect a local increase in the concentration of Cs relative to K due to the pile-up of incompatible elements in a boundary layer of melt adjacent to the crystal growth front. The addition of an aqueous solution to the Rayleigh model (i.e., the simultaneous crystallization of K-feldspars from melt and from aqueous solution) predicts high and increasing K/Cs ratios of K-feldspars that are not observed in natural rock suites, except when K-feldspars crystallize in miarolitic cavities or when primary K-feldspar recrystallizes to microcline perthite in an open hydrothermal system. In those cases, the Cs content of K-feldspars falls to nil because of the high solubility of Cs in aqueous solution and low compatibility of Cs in K-feldspar. Otherwise, the observed patterns of K/Rb or K/Cs in K-feldspar and micas in pegmatites conform to crystal-melt fractionation in which an aqueous solution plays no part. From the viewpoint of the geochemistry of Cs in pegmatites, these observations give support to the model proposed by Cameron et al. (1949) and endorsed by Jahns (1953a, 1953b).

Keywords: Cesium, Rayleigh fractionation, pegmatite, K-feldspar

INTRODUCTION

Ever since early work by Černý (e.g., Černý et al. 1985), the K/Rb and K/Cs ratios of K-feldspars (reported as a ratio of weight) and of micas have been widely used as monitors of the extent of fractional crystallization of granites and the pegmatites they produce. When graphed as K/Rb vs. Rb, K/Rb vs. Cs, or K/Cs vs. Cs, the resultant patterns exhibit exponentially decreasing trends (e.g., Roda-Robles et al. 2012; Hulsbosch et al. 2014; Marchal et al. 2014; Brown et al. 2017), or decreasing linear arrays in log-log plots (Černý et al. 1985).

Shearer et al. (1992) utilized the K, Rb, Ba, and Cs contents of K-feldspar samples from Harney Peak granite and surrounding pegmatites and compared them to a Rayleigh model for the fractionation trends across the pegmatite district. Their results are mostly compatible with Rayleigh fractionation, although they note that the rare-element pegmatites are displaced from the trends in trace-element content that link the Harney Peak granite to the tens of thousands of common pegmatites that emanate from it. Kontak and Martin (1997) observed that trace-element variations in K-feldspar from the South Mountain batholith, Nova Scotia, closely fit modeled Rayleigh fractionation trends, although the results for Cs in K-feldspar were erratic. They attributed this variability to the volatility of Cs in an aqueous solution (Carron and Lagache 1980), implying that the scatter of data reflected variable degrees of recrystallization of the primary K-feldspar and loss of Cs in an open hydrothermal system.

Roda-Robles et al. (2012) demonstrated that the K/Rb and K/Cs ratios of K-feldspars and micas in the granite-pegmatite system of Pinilla de Fermoselle, Spain, conform to a Rayleigh fractionation trend. Hulsbosch et al. (2014) plotted their analytical data for a field of pegmatites in Rwanda against modeled curves calculated by the Rayleigh equation, and they concluded that the good fit between modeled and actual values was evidence that the crystallization of K-feldspar from melt followed a Rayleigh fractionation process (Fig. 1). London et al. (2012, 2020a) likened the pattern of K/Cs in K-feldspar vs. distance from pegmatite margin to core to a Rayleigh fractionation process. London et al. (2012, 2020a) observed outliers with anomalously high-K/Cs ratios that were attributed to the recrystallization of K-feldspar in an open hydrothermal system.

In their summary of pegmatite geology, Cameron et al. (1949) concluded that zoned pegmatite bodies crystallize from their margins to center as essentially closed systems. If that zonation is fully symmetrical about the central plane of the body, then the distance from margin ($F = 1$ in the Rayleigh equation) to center ($F = 0$) is a proxy for the fraction of melt (F) that has crystallized, or $1 - F$, in the Rayleigh equation. For this reason, the fraction of melt crystallized, $1 - F$, is plotted in the figures presented here where values of K/Cs of K-feldspar are normalized to $1 - F$ based on their distance from margin to center.

In these few studies to date, the Rayleigh models and their close correspondence to observed trace-element patterns in K-feldspar apply only to fractionation between minerals and melt, because the partition coefficients utilized are derived from

* E-mail: dlondon1@memphis.edu

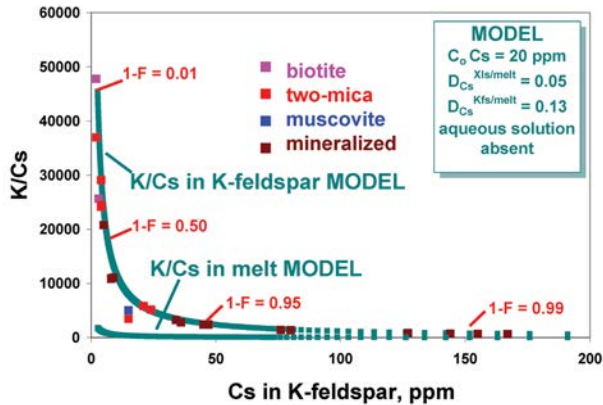


FIGURE 1. A Rayleigh model of the K/Cs ratio of K-feldspars vs. Cs in K-feldspar, and data for individual pegmatites in Rwanda from Hulsbosch et al. (2014). The labels for the types of pegmatites are from Hulsbosch et al. (2014). Modeled curves (green) show the K/Cs ratios in K-feldspar and in melt. The fraction of melt crystallized, $1 - F$, is denoted at three values on the curve for K/Cs in feldspar. See the text for the parameters of the Rayleigh model. (Color online.)

natural or experimental mineral-melt systems. The effects of a coexisting aqueous solution on the K/Cs ratio of K-feldspar have not been considered.

GOALS AND APPLICATIONS

The goal of this study is to utilize the Rayleigh equation more fully, and specifically to consider the consequences of the separation of an aqueous solution from melt on the K/Cs ratio of K-feldspar at any stage in the formation of a pegmatite body or a pegmatite group. This study models the evolution of the K/Cs ratios of melt, with and without aqueous solution equilibrated with the melt, and of K-feldspar (Kfs) crystallized from the melt only, from the melt in equilibrium with an exsolving aqueous solution, and from an aqueous solution that has exsolved from the melt. The form of the equation used is $C_i = C_0 \cdot F^{D-1}$, where C_i is the concentration of the trace element i in melt, C_0 is the initial concentration of that element at the onset of crystallization ($F = 1$), F is the fraction of melt remaining, and D is the bulk distribution coefficient for that element in the crystallizing assemblage.

The results of this study apply to two contrasting models for the internal evolution of pegmatite bodies: (1) the essentially igneous model of Cameron et al. (1949) and (2) the fundamentally aqueous model of Jahns and Burnham (1969). The models are different in another respect: Cameron et al. (1949) advocated a model of sequential fractional crystallization, which included the precipitation of pure quartz cores, the last primary unit to form in common granitic pegmatites, directly from a pegmatite-forming melt. Jahns and Burnham (1969) and Jahns (1982) fit pegmatite consolidation to a model of mineral-melt equilibrium that entailed the simultaneous crystallization of all major minerals in their eutectic proportions in the hydrous granitic system. As an economic application, the utility of the K/Cs ratio of K-feldspars to exploration for rare-element deposits in pegmatites is also assessed here. Among those ores, pollucite, nominally $\text{CsAlSi}_2\text{O}_6$, is highly sought today.

BACKGROUND

Because of its large ionic radius [mean 1.88 Å with a coordination number of 12 (Shannon 1976)] and low charge (+1), Cs is one of the most incompatible elements (incompatibility defined as $C_i^{\text{xl}}/C_i^{\text{melt}} = D_i^{\text{xl/melt}} < 1$) in all of the common rock-forming minerals, including those in which potassium is an essential structural constituent (e.g., London 2005). Partition coefficients for Cs between the common rock-forming minerals of granites and pegmatites (quartz, sodic plagioclase, K-feldspar, muscovite, and biotite) and their granitic liquids (melt) have been measured (e.g., Table 10-2 of London 2008; and sources therein), and all are less than unity. It is feasible, therefore, to calculate a bulk distribution coefficient, $D_{\text{Cs}}^{\text{xl/melt}}$, for the purposes of Rayleigh modeling that is applicable to the crystallization of typical “two-mica” (biotite-muscovite) granites and the pegmatites they spawn (Table 1).

There are few reported values of $D_{\text{Cs}}^{\text{Kfs/melt}}$ because of the very low concentrations of Cs in K-feldspar and hence the difficulty of measuring it. Icenhower and London (1996) cite $D_{\text{Cs}}^{\text{Kfs/melt}} = 0.13$ for K-feldspar synthesized from peraluminous rhyolitic melt. Partition coefficients for sanidine-glass pairs from natural peraluminous rhyolite vitrophyres range from 0.02–0.24 with a mean ($n = 12$) of 0.16 (Ren 2004). Nash and Crecraft (1985) reported comparable values (0.11–0.16) for another peraluminous rhyolite. The single value of $D_{\text{Cs}}^{\text{Kfs/melt}} = 0.13$ is employed for this model.

Cesium is highly compatible in silica-rich melts (e.g., Roy and Navrotsky 1984), where it can accumulate to weight-percent levels before achieving saturation in pollucite (London et al. 1998), the only significant and rare Cs mineral. Because of the incompatibility of Cs in minerals and the high solubility of pollucite at liquidus temperatures, Cs remains unbuffered to any appreciable extent throughout the fractional crystallization of granite-pegmatite bodies, whereas the K component of melt is constrained to a nearly constant value by the near-eutectic compositions of the granitic liquids. As a result, the K/Cs ratio of melt decreases over the course of fractional crystallization. The same is true of the principal K-bearing minerals, K-feldspar and micas, in the proportion of their crystal-melt partition coefficients.

Cesium is exceedingly incompatible in K-feldspar in equilibrium with a saline aqueous solution (aq) at elevated pressure and temperature. Values of $D_{\text{Cs}}^{\text{aq/Kfs}} = 40$ come from two relevant

TABLE 1. Rayleigh model parameters

| | Mode | D (K) | Weight ^a | Mode | D (Cs) ^b | Weight |
|---|------|---------|---------------------|------|-----------------------|--------|
| Granite bulk distribution coefficients | | | | | | |
| Qtz | 0.33 | 0.00 | 0.00 | Qtz | 0.33 | 0.00 |
| Pl | 0.36 | 0.50 | 0.18 | Pl | 0.36 | 0.00 |
| Kfs | 0.24 | 2.38 | 0.57 | Kfs | 0.24 | 0.13 |
| Bt | 0.02 | 2.47 | 0.05 | Bt | 0.02 | 0.30 |
| Ms | 0.05 | 2.40 | 0.12 | Ms | 0.05 | 0.20 |
| | | $D =$ | 0.92 | | | $D =$ |
| Pegmatite bulk distribution coefficients | | | | | | |
| Qtz | 0.34 | 0.00 | 0.00 | Qtz | 0.34 | 0.00 |
| Pl | 0.32 | 0.50 | 0.16 | Pl | 0.32 | 0.00 |
| Kfs | 0.28 | 2.52 | 0.83 | Kfs | 0.28 | 0.13 |
| Bt | 0.00 | 2.40 | 0.00 | Bt | 0.00 | 0.30 |
| Ms | 0.06 | 2.40 | 0.02 | Ms | 0.06 | 0.20 |
| | | $D =$ | 1.01 | | | $D =$ |

^a The weighted contribution of each mineral to the bulk distribution coefficient, D .

^b From Table 10-2 of London (2008).

experimental studies (Volfinger 1969; Carron and Lagache 1980). Because of its incompatibility in minerals, cesium is also widely regarded as a volatile component in aqueous solutions that might coexist with granitic liquid, but confirming data from experimental measurements are sparse. Two sources that utilized different flux-bearing, high-silica liquids at moderate pressures (200 MPa) and temperatures (650–800 °C) yielded similar values, $D_{Cs}^{aq/melt} \approx 0.2$, at <0.2 molal Cl salinity of the aqueous solution (London et al. 1988; Webster et al. 1989). Even in solutions of such low-ionic strength, $D_{Cs}^{aq/melt}$ is twice the value as for K. Values of $D_{Cs}^{aq/melt}$ rise rapidly with increasing chloride salinity of solution, from $D_{Cs}^{aq/melt} = 2.3$ at 2.0 molal Cl to ~4–7 at 3–7 molal Cl (Webster et al. 1989). For the purposes of this model, two values of $D_{Cs}^{aq/melt} = 0.2$ and 6.0 illustrate the Rayleigh trends when Cs is highly compatible or highly incompatible in silicate liquid relative to an aqueous solution.

METHODS OF THIS STUDY

Numerical modeling

A necessary condition for applying the Rayleigh equation is that equilibrium exists among melt, aqueous solution, and the surfaces of crystals, such that the chemical potential gradients of all components, including isotopes, throughout the fluid media are zero. That condition is mandated by the reliance on partition coefficients that are, or are meant to be, as close to the equilibrium of the liquidus as is possible, and by the constancy of partition coefficients anywhere in the system. In order for that to be the case, the diffusivity of all ions through a fluid medium must be rapid in relation to the rate of transfer of those ions to another medium, e.g., from melt to crystals or melt to aqueous solution. The diffusivity of ions through aqueous solutions in response to chemical potential gradients at elevated pressure is believed to be nearly instantaneous, although experimental confirmations of this behavior are almost nil (e.g., Ildefonse et al. 1979). The issue pertains to chemical equilibrium between melt and the surfaces of crystals. At their undercooled conditions of crystallization (e.g., Morgan and London 1999; London et al. 2012, 2020a, 2020b), pegmatite-forming melts possess exceedingly high viscosities on the order of 10^7 – 10^8 Pa s (London 2008). High viscosity correlates with low diffusivity of most elements (e.g., Mungall 2002), leading to boundary layer pile-up of incompatible elements (when the accumulation of excluded elements in melt due to crystallization exceeds the rate at which they diffuse away from the crystal-melt interface) and transient gradients in their chemical potentials across the melt volume.

One assessment comes from experiments in which the chemical diffusivity of alkali ions has been measured. Acosta-Vigil et al. (2012a) have observed that the diffusivity of Na and K through melts at high temperature (800 °C, 200 MPa) is essentially instantaneous in response to gradients in their own compositions or to gradients imposed by other cations with which the alkalis interact. Morgan and London (2005) found that the diffusion of Na and K through undercooled granitic melt or glass was instantaneous (i.e., equilibrated with aqueous solution and crystals at least on the scale of minutes) down to 515 °C at 200 MPa. In a comparison of crystal-melt partitioning in natural glass-mineral pairs, Acosta-Vigil et al. (2012b) ascertained that the distributions of the alkalis, including Cs, came closest of all elements to their published equilibrium partition coefficients. These results would justify a Rayleigh model for alkalis in natural granite-pegmatite systems.

However, the diffusivity of Cs through melt is the lowest of all the alkali ions, which Roselieb and Jambon (1997) attribute to the large ionic radius of Cs. London and Morgan (2012) documented a pronounced boundary-layer pile up of Rb, Cs, and other incompatible ions (B, F) along a crystallization front that was achieved by liquidus undercooling of a hydrous melt that was derived from the Macusani obsidian. In that case, the Cs content of K-feldspar that crystallized from the melt will reflect the elevated concentration of Cs in the boundary layer liquid, not that of the bulk melt (see Smith et al. 1955). The result would be that the K/Cs and K/Rb ratios of the K-feldspars fall more rapidly than the Rayleigh model would predict but approach the Rayleigh trend toward the end of crystallization as the system reacts toward the equilibrium of the liquidus. For this scenario, the values of K/Cs and K/Rb ratios in K-feldspar might crossover (i.e., exceed) the Rayleigh trend at the end of crystallization as required by the conservation of mass.

The individual partition coefficients for some mineral-fluid pairs change with the composition of the mineral, of the nutrient solution (melt or aqueous), or with temperature. Bulk distribution coefficients may vary as a mineral assemblage evolves. These factors place additional and well-known limitations on the application of the Rayleigh equation to chemically and mineralogically complex systems. Mineral assemblages and mineral compositions, however, change only slightly from the “two-mica” biotite-muscovite granites to their more fractionated pegmatite bodies. Cesium is so incompatible in rock-forming minerals that its partition coefficients are unlikely to vary over the course of cooling and crystallization. It is for these reasons that the K/Cs ratio of K-feldspar offers a useful test of the applicability of the Rayleigh fractionation model for pegmatites and a meaningful assessment of the roles of melt and aqueous solution in the internal evolution of granitic pegmatites. The Rayleigh models developed here with their input parameters are available as Online Materials¹ Appendix I. Details of the parameters used are given below where appropriate.

New analyses of K/Cs in K-feldspar

A reconnaissance study included here reports the K/Cs ratio of K-feldspars in three subsurface drill intersections from margin to margin across the General Electric Southeast pegmatite on Hodgeon Hill, near Buckfield, Oxford County, Maine. Inclined drill holes intersected the pegmatite at an angle of ~45° to the pegmatite contacts at three different depths (Fig. 2). A surface adit into the pegmatite to a distance of ~20 m provides wall-to-wall exposure across the dike. The body strikes east-west with a nearly vertical dip and a thickness of ~5 m. Wall zones on both margins consist of massive, medium-grained (2–3 cm) granitic pegmatite with minor biotite. A thin and sporadic band of aplite was exposed along the northern contact of the dike. Symmetrical intermediate zones possess strongly unidirectional solidification texture (UST) in which muscovite crystals up to 60 cm in length form linear ribbons oriented perpendicular to the contact. The core margin is marked by an abundance of tourmaline crystals that exhibit UST and expand toward the core. The core consists of blocky white-beige perthitic K-feldspar with interstitial smoky quartz and minor lenses of pure smoky quartz. Mining by Freeman Resources LLC encountered pods of pollucite, each ~0.1–0.3 m³ in volume, with minor montebrasite (LiAlPO₄OH) and Cs-rich beryl along the center line of the pegmatite at approximately every 3 m of mining distance into the adit. Other than traces of montebrasite and rare lepidolite rims on muscovite at the core, the pegmatite contains no lithium-rich minerals.

The pegmatite was sampled by recovering chip composites at 10 foot (~3 m) intervals of percussion drilling. The recovery method resulted in a thoroughly mixed sample at each interval of collection. Samples of each interval were split and hand-picked for K-feldspar fragments. Each K-feldspar sample consisted of ~15–30 fragments weighing ~15–230 g in total. These were submitted for analysis by Actlabs (Ancaster, Ontario, Canada) using their “4 Litho-quant” analytical package. In that 20-sample set, the average feldspar composition is Or₆₁Ab₃₆An₀₂, with a uniform phosphorus content of 0.26 (1σ = 0.06) wt% P₂O₅ (Online Materials¹ Appendix II). The standard deviations were 1.1 wt% for Na₂O and 1.7 wt% for

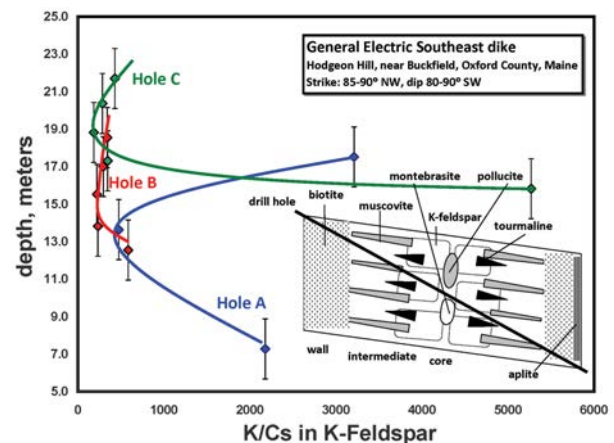


FIGURE 2. A plot of K/Cs in K-feldspar vs. depth in the holes that represent three oblique intersections from margin to margin across a single dike, the General Electric Southeast, near Buckfield, Maine. (Color online.)

K₂O. In contrast, electron microprobe analyses (Online Materials¹ Appendix II) that were restricted to the perthitic portions only yielded an average composition of Or₉₃Ab₀₇An₀₀ and standard deviations of 0.25 wt% for Na₂O and 0.33 wt% for K₂O (N = 450). Comparison of the two data sets indicates that the hand-picked sample was contaminated to various degrees by admixed albite as accidental grains and as inclusions within perthite, as this is the norm for pegmatitic K-feldspars (London et al. 2020a, 2020b). Therefore, the K/Cs ratios of the feldspars represent a close approximation to their true value in K-feldspar because albite is not a host for either element. The individual concentrations of K and Cs in the hand-picked sample, however, are not representative of K-feldspar.

The K/Cs ratio of K-feldspar crystallized from melt

Granite to pegmatites. The granite-pegmatite system of the model is a “two-mica” muscovite-biotite granite, for which the bulk distribution coefficient for Cs is 0.05 (Table 1; Online Materials¹ Appendix I). The bulk distribution coefficient for K is derived by dividing the wt% K elemental in each end-member mineral by the concentration of K in the melt. That value is 41 489 ppm K for a typical granitic liquid of metasedimentary (S-type) origin (equivalent to the average of 5 wt% K₂O cited by Chappell and White 2001). The resulting bulk distribution coefficient for K is 0.92, which reflects the nearly invariant composition of crystals and melt for liquids that crystallize close to their eutectic temperatures. For the Rayleigh model, the initial Cs content of melt is 20 ppm. This is high in relation to subduction-related rhyolite obsidians (average 6 ppm Cs; Macdonald et al. 1992), but appropriate for partial melts that are derived from originally muscovite-rich schists (average 23 ppm Cs; Acosta-Vigil et al. 2010).

With these parameters, the Rayleigh equation was run for the evolution of K and for Cs in melt. The K/Cs of melt is the quotient of these two values at each iteration of the Rayleigh equation. The Cs content of K-feldspar is 0.13·Cs in melt. The K/Cs ratio of the feldspar is the quotient of a constant K content (119245 ppm K, which corresponds to a typical composition of Or₉₃) divided by the product of the calculated Cs content of the K-feldspar.

Figure 1 is a plot of K/Cs vs. Cs of K-feldspar using these modeled parameters. Plotted against that are analyses from the Rwandan pegmatites that were the source data for Figure 2b of Hulsbosch et al. (2014). Despite small differences in the input parameters of initial Cs content, modal mineralogy, and partition coefficients, the correspondence of modeled and actual values affirms that the compositions of K-feldspars in the Rwandan pegmatites closely approached a Rayleigh fractionation trend for crystallization from the melt, as Hulsbosch et al. (2014) concluded.

Within pegmatites. For the pegmatitic system modeled (Table 1; Online Materials¹ Appendix I), the bulk distribution coefficient for Cs is 0.05. With a slightly different modal assemblage, the bulk distribution coefficient for K, $D_K^{Xts/melt} = 1.01$, the value of unity that follows from eutectic crystallization. The composition of the K-feldspar is adjusted to Or₉₀, which is more representative of pegmatites than of granites. As before, an aqueous solution is not present in the model.

Values of K/Cs of K-feldspar come from two thin subhorizontal pegmatites, cited as the Swamp and Phantom dikes, from Ramona, California (London et al. 2012, 2020a). Both dike sections are ~40–50 cm across from the footwall contact to or near the center of each dike. Neither dike is visibly miarolitic. Other than feldspars and quartz, the pegmatites contain accessory tourmaline and trace amounts of muscovite and garnet. The average Cs content of the Swamp cross section is 8 ppm Cs. The average Cs of the Phantom cross section is 20 ppm Cs. In the Rayleigh model, however, the initial concentration of Cs in melt is set at 75 ppm to scale the modeled values to those of the actual pegmatites. It is possible that the footwall portions of the dikes do not represent the bulk compositions of the pegmatites because the hanging wall portions along the center line of each dike contain an appreciable fraction of the K-feldspar in each dike (Fig. 4 of London et al. 2012). Compositions of garnet and of plagioclase indicate that crystallization up from the footwall preceded and advanced faster than did crystallization down from the hanging wall contact, which explains why the dike center lines are displaced toward the top of these and similar thin, layered pegmatite bodies (Morgan and London 1999; London et al. 2012). In that case, crystallization from margins to the dike center was more sequential than contemporaneous, and the portions of dikes above and below the center line are not mirror images of one another (e.g., see Fig. 26 of London 2014).

In Figure 3, the modeled values for K/Cs of melt and of feldspar as calculated above are plotted along with the K/Cs of K-feldspars from the Swamp and Phantom dikes against the fraction of melt crystallized, which is proportional to the distance from margin to center of each dike on the premise that the dikes are fully crystallized from both margins at their centers. The plot for the Phantom dike terminates

at $1 - F = 0.8$ because this cross section ended ~10 cm short of the true dike center. The K/Cs ratios of K-feldspars in the two dikes initially fall more rapidly than the Rayleigh model predicts. The tails of the curves for the pegmatitic K-feldspars approach the final values of the Rayleigh trend or crossover it.

The K/Cs ratio of K-feldspar crystallized from melt and aqueous solution

The additional effect of an aqueous solution in equilibrium with melt and crystals is modeled as follows. In the Rayleigh model, the initial Cs content of melt is 100 ppm. First, the Rayleigh equation is solved for Cs in melt vs. $1 - F$, wherein the bulk distribution coefficient is the same as $D_{Cs}^{ag/melt}$ (values of 0.2 and 6.0 in this study). In this first step, the value $1 - F$ corresponds to the fraction of aqueous solution in the system of melt-aqueous solution and to the fraction of melt crystallized, as the mass of exsolved aqueous solution increases in response to crystallization of the melt. The resultant values of Cs are those of the melt. The melt composition is then adjusted for the small fraction of Cs that is removed by crystallization. Following this step, the Cs content of the aqueous solution is the product of Cs in melt times the value of $D_{Cs}^{ag/melt}$ (0.2 or 6.0) at each iteration of $1 - F$ in the Rayleigh equation. The K/Cs ratio of K-feldspar crystallized from the melt is the constant K content for Or₉₀ (126259 ppm) divided by the Cs concentration in K-feldspar, which is 0.13·Cs in melt. The concentration of Cs in feldspar crystallized from aqueous solution is the product of the Cs content of aqueous solution times the reciprocal of the published partition coefficient (Volfinger 1969; Carron and Lagache 1980), i.e., $D_{Cs}^{Kfs/aq} = 0.025$. The elemental K content of the feldspar is again held constant at Or₉₀. The K/Cs ratio of K-feldspar crystallized from aqueous solution is that K value divided by the concentration of Cs. The resultant values are plotted against $1 - F$ as described above. By this sequence of steps, the Rayleigh models simulate the K/Cs ratios of K-feldspars that crystallize simultaneously from melt and from aqueous solution as the fraction of crystallization and the fraction of aqueous solution increase with $1 - F$.

In Figure 4a, the fractionation trend for K/Cs of K-feldspar crystallized from melt in equilibrium with a low-salinity solution and $D_{Cs}^{ag/melt} = 0.2$ is similar in slope and form to the aqueous solution-absent case (e.g., the modeled values in Fig. 3) because the loss of Cs to aqueous solution is negligible over the course of crystallization. The K/Cs ratio of K-feldspar crystallized from aqueous solution, however, is exceedingly and unrealistically high in relation to the values that are reported from natural samples in this study and the others cited.

In Figure 4b, the K/Cs ratios of K-feldspar crystallized from melt and from aqueous solution of high salinity, with $D_{Cs}^{ag/melt} = 6.0$, increase exponentially as crystallization proceeds. This is because the large partition coefficient, $D_{Cs}^{ag/melt}$, depletes the melt in Cs as the mass fraction of aqueous solution increases. The concentration of Cs in aqueous solution also falls as the mass of that solution increases. The feldspars crystallized from melt or from aqueous solution, therefore, record a progressive increase in their K/Cs ratios, as most of the Cs winds up in the aqueous solution.

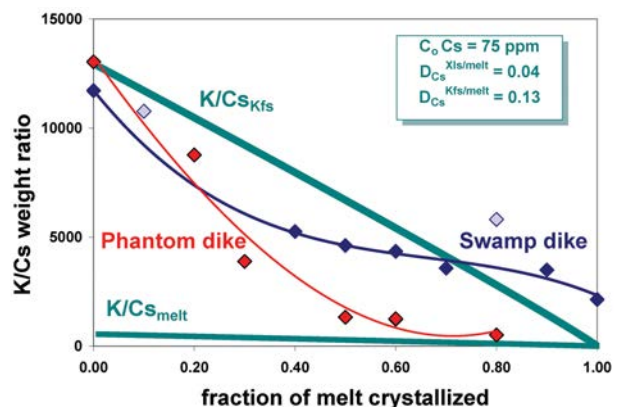


FIGURE 3. A Rayleigh model (green) of K/Cs in melt and in K-feldspar, and K/Cs ratios of feldspars from two pegmatite dikes near Ramona, California, plotted against $1 - F$, fraction of melt crystallized. See the text for details of the Rayleigh model. For the Swamp dike, two outlier values are illustrated in lighter blue. (Color online.)

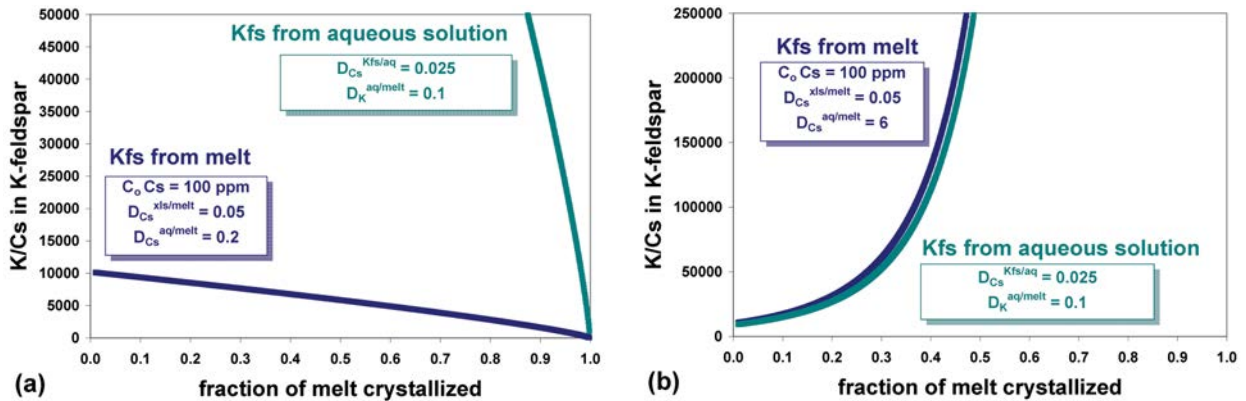


FIGURE 4. (a) Rayleigh models of the K/Cs ratio of K-feldspars crystallized simultaneously from melt (blue) and aqueous solution (green) vs. the fraction of melt crystallized for the condition of $D_{Cs}^{aq/melt} = 0.2$, wherein Cs is highly compatible in melt compared to aqueous solution. (b) Rayleigh models of the K/Cs ratio of K-feldspars crystallized simultaneously from melt (blue) and aqueous solution (green) vs. the fraction of melt crystallized for the condition of $D_{Cs}^{aq/melt} = 6.0$, wherein Cs is highly compatible in aqueous solution compared to melt. (Color online.)

DISCUSSION

The record of K/Cs in pegmatitic K-feldspar

The high incompatibility of Cs in nearly all of the principal rock-forming minerals (except cordierite; Evensen and London 2003) means that its concentration in partial melts is unbuffered by subsequent crystallization. It is, therefore, a useful diagnostic of the parental source of pegmatites, which are the products of protracted fractional crystallization of larger igneous bodies (e.g., Černý et al. 1985; Černý 1991; London 2008, 2019). Černý (1991) associated the Cs-rich pegmatites (his LCT family, for Li-Cs-Ta) with granites that are sourced from previously unmelted metasedimentary rocks, which are mostly marine deposits of black shale and arkosic turbidite. The Cs-enriched signature of this source arises from the adsorption and incorporation of Cs in the micaceous minerals, including clays, sericite, and chlorites (see London 2016, 2018 and citations therein). Anomalously high concentrations of boron and phosphorus in the LCT family of pegmatites also originate with their inclusion in marine sediments.

Gordiyenko (1971) made the initial observations that the Rb and Cs contents of K-feldspar increase inward within zoned pegmatite dikes. Petr Černý demonstrated that the plot of K/Cs or K/Rb vs. Cs of K-feldspars follows an exponentially decreasing trend from the granites to their most evolved and distal rare-element pegmatites (Černý 1994; Černý et al. 1985). As is evident from this study, that trend is a result of the fractional crystallization of K-feldspar from the melt, and the K-feldspars mostly preserve it faithfully, even as recrystallized perthitic microcline. It is for this reason that London et al. (2012, 2020a, 2020b) concluded that feldspar solvus thermometry can be a valid record of the original temperature of crystallization of primary feldspars once the compositions of the perthitic K-feldspar are properly analyzed and integrated.

To be sure, not all K-feldspars in granites and pegmatites preserve their initial igneous compositions, but the K/Cs ratio and total Cs contents are sensitive monitors of alkali loss in an open hydrothermal system. London et al. (2012a) pointed to outliers (light blue diamonds of Fig. 3) of high K/Cs as indicative of feldspars that have lost Cs, and therefore have recrystallized

to some extent in an open system. In Figure 3 of Parsons et al. (2009), two populations of alkali feldspar—one with elevated Cs contents, the other with values below detection limits—from the Klokken granite intrusion in South Greenland, reflect their igneous and hydrothermal origins, respectively.

The observed patterns of K/Cs and K/Rb in K-feldspar are mirrored by the micas from granites and pegmatites. The partition coefficients for Rb and Cs are nearly identical in K-feldspar and micas over a range of compositions of melt and aqueous solution (Volfinger 1969). The primary-appearing coarse-grained mica record the same exponentially decreasing K/Rb and K/Cs ratios that reflect their crystallization from silicate liquid in the pegmatites studied to date (e.g., Černý 2005; Canosa et al. 2012; Roda-Robles et al. 2012; Marchal et al. 2014; Neiva 2014). What holds true for the K-feldspars holds true for the micas, as Hulsbosch et al. (2014) demonstrated for K/Rb and K/Cs ratios in primary K-feldspars and micas in pegmatites from Rwanda: they follow Rayleigh fractionation trends for their crystallization from the silicate melt.

An assessment of case studies

Several of the pegmatites mentioned here deserve some discussion. The Tanco pegmatite, Manitoba, is included because it is an archetype of the LCT family of rare-element pegmatites and their associated ores, its feldspars are well studied, and it is essentially flat-lying. The K/Cs data set for the General Electric Southeast pegmatite, Maine, is unique because it spans a vertical pegmatite from border to border. The Swamp and Phantom dikes, California, are among the very few for which K/Cs ratios are available from margin to core, and for which the temperatures of their crystallization are well constrained (London et al. 2012, 2020a). Feldspars that crystallize in miarolitic cavities and that recrystallize with the formation of perthitic microcline bear upon the role of aqueous solutions in the late stages of pegmatite consolidation.

Tanco pegmatite, Manitoba. On average (Table 2 and Figs. 2 and 7b of Brown et al. 2017), blocky K-feldspars in the Tanco pegmatite, Manitoba, exhibit the decrease in K/Cs from border to late units that follows upon chemical fractionation and crystallization from a melt. That trend begins to reverse itself in zone 90 (from K/Cs = 50 to K/Cs = 775, Fig. 2c of Brown et al. 2017),

which is dominated by fine-grained lepidolite and is regarded as the last mappable unit to have crystallized in the pegmatite after the pollucite zone 80 (Černý 2005; Stilling et al. 2006). Brown et al. (2017) identified five textural-paragenetic types of what they term “metasomatic” K-feldspars at Tanco, implying that these feldspars formed by replacement of a previous mineral or mineral assemblage through the chemical exchange in an open hydrothermal system. Similar generations of chemically complex and heterogeneous late-stage K-feldspar have been described elsewhere (e.g., Teertstra et al. 1999). The “metasomatic” feldspars are fine grained and exceedingly rare. In a few samples, the concentrations of Rb and of Cs in such feldspars are among the highest measured, but most of the reported analyses are below detection levels and reported as zero values (Table 3 of Brown et al. 2017). Their phosphorus contents include a few values similar to those of the primary blocky perthitic microcline found in these and other peraluminous pegmatites, most of which possess >0.3 wt% P₂O₅ (London et al. 1990). However, the large majority of the analyses of “metasomatic” feldspars yield undetectable phosphorus, which is also characteristic of K-feldspars from miarolitic cavities in otherwise phosphate-rich pegmatites (London et al. 2012b). Hydrothermal K-feldspar of adularia habit (Type 6 of Brown et al. 2017) in small and rare vugs is extremely depleted in Cs relative to the primary perthitic microcline in the late-forming zones (Černý and Chapman 1984; Brown et al. 2017). The reversal in the decreasing trend of K/Cs can be explained if some K-feldspar from zone (90), the “metasomatic” feldspars, and adularia in late-stage vugs reflect the imprint of increasing K/Cs that results when the feldspar crystallizes or recrystallizes from an aqueous solution.

General Electric Southeast pegmatite, Maine. The K/Cs ratios of K-feldspars (Fig. 2) exhibit increasing fractionation from both margins of the dike to its core, as might be expected from the bilateral symmetry that is evident in the surface adit of the pegmatite. The symmetry of the curves in Figure 2 is consistent with the model proposed by Cameron et al. (1949), wherein crystallization of the melt proceeds more or less simultaneously from both margins to the centers of dikes. Such zonation is typical of steeply dipping pegmatite bodies, which formed a large proportion of the pegmatites studied by Cameron et al. (1949). The study also demonstrated that exploration based on percussion drilling, which is much less costly than core drilling, can recover samples that reflect the spatial chemical variations in pegmatites.

Swamp and Phantom pegmatites, California. Plots of K/Cs in K-feldspar vs. distance from margin to center for the Swamp and the Phantom pegmatites deviate from the Rayleigh model with ratios that are initially lower (more fractionated) than predicted. These might result from the pile-up of Cs in a boundary layer liquid, as has been observed in experiments, leading to lower K/Cs ratios in the feldspars. The K/Cs values of both dikes approach the Rayleigh trend toward the dike centers, which could be interpreted as an approach to crystal-melt equilibrium as crystallization proceeded. The feldspars also evolve from non-perthitic mixed orthoclase-microcline to coarsely perthitic maximum microcline, and from graphic intergrowths to monophasic feldspars from margins to core (London et al. 2012, 2020a). The final K-feldspars from the Swamp dike possess slightly higher K/Cs than the Rayleigh model. This is a necessary consequence of the conservation of mass in the pegmatite body, as more Cs

was removed, relative to the Rayleigh model, at early stages of crystallization. The trend in the Phantom dike does not cross the Rayleigh plot, but that dike was not fully sampled to its center line.

The Rayleigh model also can be utilized to calculate the initial concentration of Cs of the melt that would be necessary to achieve the observed K/Cs ratios of the first-formed K-feldspars if those feldspars crystallized from an aqueous solution rather than a melt. In that case, the bulk distribution coefficient, $D_{Cs}^{ls/eq}$, for Cs is 0.004 (partition coefficients for micas from Volfanger 1969). With a bulk distribution coefficient that is approximately an order of magnitude lower than that between crystals and melt, the consequent Cs content of melt needed to reproduce the compositions of the initial feldspars in the Swamp and Phantom dikes is ~800 ppm Cs, about an order of magnitude greater than the modeled value in Figure 3. Starting with that initial concentration of Cs and the minuscule value of $D_{Cs}^{ls/eq}$, that melt would reach 2600 ppm Cs, the concentration of Cs in the bulk composition of the pollucite-rich Tanco pegmatite (Stilling et al. 2006), at just 70% of crystallization. Were this case true, a great many of otherwise common pegmatites would contain pollucite. This conclusion is neither plausible nor consistent with the unfractionated compositions of the Swamp and Phantom dikes (Table 2 of London et al. 2012).

The plot of K/Rb in K-feldspar vs. distance from margin ($1 - F$) for the Phantom dike (Fig. 14 of London et al. 2020a) more closely approaches the quasi-linear plot of a Rayleigh model than does Cs. Two factors might influence this trend: (1) the higher compatibility of Rb compared to Cs in K-feldspar (Icenhower and London 1996), and (2) the higher diffusivity of Rb compared to Cs in melt (Roselieb and Jambon 1997).

Miarolitic pegmatites. The Cs content of K-feldspars in miarolitic cavities is practically unstudied. As noted above, K-feldspar of adularia habit in small and rare vugs at Tanco has essentially no Cs (Černý and Chapman 1984). Miarolitic K-feldspars from two pegmatites in Argentina were at or below a detection threshold that was reported as 0.01 wt% Cs₂O (Černý et al. 2003). A global survey (London et al. 2020b) found the Cs content of K-feldspars from 12 miarolitic pegmatites to lie below detection by electron microprobe analysis (0.05 wt% Cs₂O calculated at 3σ above mean background). This suite includes samples from the pegmatites of the Little Three mine, Ramona, California (the same locality as the Swamp and Phantom dikes), where quartz and topaz from miarolitic cavities contain daughter minerals including pollucite, ramanite [CsB₅O₆(OH)₄·2H₂O], and an unnamed Cs arsenate (London et al. 2012) in fluid inclusions of low-ionic strength (see column Tm_{icc} in Table 10 of London et al. 2012). Other than its occurrence as a daughter mineral within fluid inclusions, pollucite has not been documented in any of those dikes.

Subsolidus recrystallization to perthite

London et al. (2012, 2020b) noted that although much of the blocky K-feldspar in the southern California pegmatites is perthitic microcline, that recrystallization mostly occurred without the loss of Cs to an aqueous solution. That is not to say that an aqueous solution was not involved in the transformation to perthitic microcline, but that the recrystallization of the original K-feldspar occurred in a closed system in which the mass fraction of aqueous solution to K-feldspar was negligible.

Pegmatites retain their original igneous compositions and structures of K-feldspars more faithfully than do granites because pegmatites possess too little thermal mass to circulate aqueous solutions through solidified rock (e.g., Neves and Godinho 1999; London 2008), whereas granites can sustain prolonged hydrothermal interaction. The proportionately large population of Cs-depleted feldspars in granite reported by Parsons et al. (2009) and noted by Kontak and Martin (1997) can be understood on this basis. Such Cs-depleted feldspars are rare in pegmatites, except at the latest, miarolitic stage, and, where noted as outliers in the overall trend of chemical fractionation of the blocky, primary K-feldspars.

The occurrence of Cs-rich aqueous fluid inclusions with Cs-poor feldspars within miarolitic cavities of pegmatites, intense Cs metasomatism adjacent to pollucite-bearing pegmatites (discussed below), and the complete loss of Cs in K-feldspar that has recrystallized in an open hydrothermal environment attest to the high solubility of Cs in aqueous solution (i.e., $D_{\text{Cs}}^{\text{aq/melt}} > 1$, $D_{\text{Cs}}^{\text{ag/Kfs}} \gg 1$). To that extent, the evidence indicates that if a pegmatite-forming melt crystallizes with a coexisting and increasing fraction of aqueous solution, then the K/Cs ratios of all K-feldspars should follow an evolutionary path like that of Figure 4b. It is the reverse of the solely magmatic trend that the primary K-feldspar records.

The K/Cs ratio of K-feldspars as a prospecting tool

Cesium in the form of a Cs-formate solution is in high demand as a component of the dense mud used in deep drilling for petroleum and natural gas (e.g., Saasen et al. 2002). At present, pollucite represents the only commercial source. Even in pollucite-bearing pegmatites, the mineral constitutes <1 vol% (Stilling et al. 2006). The demand for ore and the rarity of its occurrence creates a rationale to discriminate those few pegmatites that might contain pollucite from the many that do not. The K/Cs ratios of K-feldspars might be one means of assessment.

The K/Cs ratios of K-feldspars associated with the pollucite zone 80 of the Tanco pegmatite cluster close to ~50 (Brown et al. 2017). The K/Cs ratios of K-feldspars in the outer zones 10, 20, and 40, are higher, but they mostly span the full range of values from ~1600 to 50 (Brown et al. 2017). At the General Electric Southeast pegmatite, all three drilled intersections yield a K/Cs ratio of K-feldspar that is ~183–474 at the core of each pegmatite transect. The highest value, 2177, lies at a margin of the dike. These values are about an order of magnitude greater than those from the Tanco pegmatite. Nonetheless, both pegmatites—Tanco and General Electric Southeast—are equally enriched in pollucite (Stilling et al. 2006, and author's unpublished field data). The K/Cs ratios are meaningful, however, only in relation to the K/Cs ratio of K-feldspar in pegmatites that are less fractionated and that lack pollucite. As examples, the K/Cs ratios of K-feldspar at the interior ends of the Swamp and Phantom dike sections are ~500 and 2100, respectively.

The Cs concentration that is necessary to saturate hydrous granitic melt in pollucite falls sharply with decreasing temperature (London et al. 1998). This variable—the temperature of crystallization of the pegmatite-forming melt—adds another measure of uncertainty to the significance of the K/Cs ratios of the K-feldspars as indicators of the probability of finding pol-

lucite in a pegmatite body. Although the ratios among K, Rb, and Cs in alkali feldspars and micas point in the direction of increasing fractionation across a pegmatite field or within a body, they are not yet definitive for distinguishing pollucite-bearing pegmatites from those that lack it.

At Tanco, the late-stage feldspars and the ensuing hydrothermal alteration of host rocks point to the involvement of an aqueous solution toward the end of crystallization in the pegmatite, and to high solubility and high mobility of Cs in that aqueous solution. Morgan and London (1987) observed that the metasomatic alteration that surrounds the Tanco body mirrors the distribution of the latest-formed primary units within the pegmatite. They concluded that all of the primary units, including the pollucite bodies, were solidified before the egress of an aqueous solution out of the pegmatite. A pervasive alteration of host metagabbro to Rb- and Cs-rich zinnwaldite is pronounced wherever large masses of pollucite are concentrated in the pegmatite. Cesium concentrations averaged 1.46 wt% Cs₂O in the metasomatic zinnwaldite (Morgan and London 1987). Approximately 13% of the original Cs content of the pegmatite was conveyed to the adjacent host rocks (Morgan and London 1989). The late-stage metasomatism of host rocks, which carries the chemical signature of the last-formed mineral assemblages, mirrors the reversal in the K/Cs ratios of the latest hydrothermal feldspars in the pegmatite (Brown et al. 2017).

An equally large and fractionated pegmatite (Lower Tanco) beneath the main upper one possesses no known pollucite except traces along its western extremity. A broad (tens of meters) and pervasive zone of exceedingly Cs-rich metasomatic dark mica that has replaced metagabbro extends off the east end of the body. The aqueous solution responsible for the metasomatic alteration emanated from or through a brecciated aplite within the pegmatite. The Lower Tanco pegmatite appears to have achieved H₂O saturation of melt earlier than the upper body, prior to the crystallization of pollucite, with the result that most of the Cs was transferred from the pegmatite to the reactive host rocks. Other examples of intense wallrock metasomatism in which Cs has been conveyed by aqueous solution to host rocks, where is it sequestered by the crystallization of Cs-rich “biotite,” are well documented (e.g., Royzenman 1982). The spatial correlation of an aureole of Cs-rich mica might augur the location of pollucite mineralization more reliably than do the pegmatitic feldspars. Conversely, a large aureole of Cs-rich mica might signify that the loss of Cs is so extensive that pollucite is not likely to be present in the source pegmatite.

IMPLICATIONS

The Rayleigh models presented here, together with the ratios among K, Rb, and Cs in alkali feldspars and micas, have these implications for understanding the internal differentiation of pegmatites.

- Variations of K/Rb and K/Cs vs. Rb or Cs generally follow Rayleigh fractionation trends for the crystallization of K-bearing minerals from silicate liquid. Both ratios decrease from source granites to their most fractionated pegmatites and from the margins of pegmatites to their innermost primary unit. The K/Cs ratio of K-feldspar initially decreases

more rapidly than the Rayleigh model predicts for two dikes in California (London et al. 2012, 2020a), which can be attributed to the accumulation of Cs relative to K in a boundary layer of liquid along the crystallization front. The K/Cs ratios of those K-feldspars converge on the Rayleigh fractionation trend, and one crossed over that trend as crystallization advanced toward the centers of the dikes. Both results can be interpreted to mean that K-feldspar and melt more closely approached a state of chemical equilibrium as crystallization advanced inward. The textures of the feldspars are consistent with this interpretation.

- If Cs is not volatile in a system of melt-aqueous solution (Fig. 4a), then the values of K/Cs vs. Cs for K-feldspar that crystallizes from the melt are essentially those of the aqueous solution-absent model. In that case, however, K-feldspar that crystallizes simultaneously from a coexisting aqueous solution will have essentially no Cs and exceedingly high K/Cs because of the large partition coefficient, $D_{Cs}^{aq/Kfs}$.
- If K-feldspar in the two dikes from California crystallized from melt components via their dissolution into and through an aqueous solution that wetted the surfaces of crystals, then the Cs content of the bulk melt needed to reproduce the K/Cs ratios of the first-formed feldspars are implausibly high.
- If Cs is volatile in a system of melt-aqueous solution (Fig. 4b), then all K-feldspars, whether crystallized from the melt or from the aqueous solution, will exhibit trends of increasing K/Cs (depletion in Cs) as the small quantity of Cs partitions into an increasing mass of aqueous solution. None of the sources of data for feldspars or micas cited here conforms to this trend, except in the very late stages of pegmatite consolidation when miarolitic cavities form and when subsolidus recrystallization occurs in an open hydrothermal system.

For pegmatite paradigms in the context of Cs geochemistry, Cameron et al. (1949) remains the most comprehensive and authoritative publication of pegmatite geology. That summary, which included R.H. Jahns as the second author, attributed the internal features of zoned pegmatites to the fractional crystallization of granitic melt from the margins of a body to its center. Their evidence for fractionation crystallization included the highly directional growth of minerals from margins to center and systematic changes in mineral habits and mineral assemblages with position within a pegmatite body. They recognized fracture-controlled replacements of minerals in the outer zones of pegmatites as reactions between early-formed minerals with later, more fractionated melt with which the outer pegmatite zones were not in equilibrium.

Cameron et al. (1949) also cited a systematic decrease in the anorthite content of plagioclase (p. 101–102) in support of a fractional crystallization model, but their data were not published. Detailed profiles of the anorthite content of plagioclase with distance from margin to center are now available (London et al. 2012, 2020a), and they bear out all of the trends mentioned by Cameron et al. (1949).

Cameron et al. (1949) hypothesized that the increasing size of crystals from margin to center arose from a reduction in the viscosity of the melt as “hyperfusibles” (p. 105)—incompatible components that act as fluxes in the melt—became concentrated

in the “rest-liquid.” As such, they viewed the giant crystals found in the innermost zones to be the products of crystallization from a melt. Cameron et al. (1949) relegated an aqueous solution to a minor role in the subsolidus alteration of primary minerals, which they and others (e.g., Jahns 1953b; Heinrich 1953) put at generally <1 vol% of any given pegmatite body. Jahns (1953a, 1953b) advocated these conclusions, taking text verbatim from Cameron et al. (1949) in his first academic publications.

Jahns (1955) subsequently invoked an aqueous fluid as the principal agent that promoted the formation of pegmatites as opposed to granites. That hypothesis, which was fully presented by Jahns and Burnham (1969) and Jahns (1982), relegated the silicate melt to a mass that was redistributed via diffusion through and buoyant ascent of the aqueous solution. Ever since, the occurrence of pegmatites has been generally regarded as a priori evidence that an aqueous solution has exsolved from an H₂O-saturated granitic liquid, and the pegmatitic stage marks the onset of exsolution of that aqueous solution.²

Jahns and Burnham (1969), Jahns (1982), and R.H. Jahns (personal communication, 1982) envisioned that the melt dissolves into an aqueous solution that forms an interconnected and continuous film along crystal surfaces. Chemical fractionation occurs between the melt and aqueous solution, such that the crystals that grow via “nourishment” (Jahns and Burnham 1969; p. 856) from the aqueous solution become progressively enriched in normally rare and incompatible elements (see Fig. 2 of Jahns 1982). This is precisely the scenario that is captured by the Rayleigh models of Figure 4, wherein the aqueous solution might be regarded as an interface between the melt and the crystals that grow from it, whose values of $D_{Cs}^{Kfs/aq}$ are those of the crystal-aqueous solution equilibrium. Figures 4a and 4b indicate that the K/Cs ratios of K-feldspars that crystallize from an aqueous solution will be unrealistically high. Conversely, the Cs concentration of the melt would have to be unrealistically high to reproduce the observed K/Cs ratios of K-feldspars if these were crystallized from the aqueous solution. Rather than enriching K-feldspar in Cs as Jahns and Burnham (1969) envisioned, crystallization from an exsolving aqueous solution would cause depletion of Cs in the K-feldspar.

Based on what is evident from field and experimental data, Cs behaves as a volatile component, meaning it is concentrated in aqueous solution over crystals or melt. The Rayleigh modeling presented here shows that if Cs were partitioned in favor of the aqueous solution ($D_{Cs}^{aq/melt} > 1$), then all feldspars, whether grown from melt or aqueous solution, would become progressively depleted in Cs as crystallization proceeds (Fig. 4b). That is not the case: the patterns of K/Rb or K/Cs in the primary, coarsely crystalline K-feldspar and micas in pegmatites conform to crystal-melt fractionation in which an aqueous solution played no part. The negligible Cs contents of K-feldspars that form in miarolitic cavities and by the subsolidus replacement of blocky primary crystals are consistent with feldspar precipitation from an aqueous solution in which Cs is highly compatible and mobile. Those Cs-depleted feldspars, however, appear only in the very latest stages of primary and subsolidus crystallization of pegmatites. From the viewpoint of the geochemistry of Cs in pegmatites, these observations give support to the model proposed by Cameron et al. (1949) and endorsed by Jahns (1953a, 1953b).

ACKNOWLEDGMENTS AND FUNDING

Niels Hulsbosch provided data for the Rwandan pegmatites used in Figure 1. Canada Sinomine Resources Inc. permitted the release of unpublished information regarding the Lower Tanco pegmatite body, Manitoba, and analyses of feldspars from the General Electric Southeast pegmatite, Maine. Gary Freeman (Freeman Resources LLC) provided samples, access, and information regarding the pegmatites of Hodgeon Hill, Maine. I thank Mona-Liza Sirbescu, Callum Hetherington, and Cal Barnes for their constructive reviews and Cal Barnes for editorial handling. This study was supported by the National Science Foundation (Grant EAR-1623110).

REFERENCES CITED

- Acosta-Vigil, A., Buick, I., Hermann, J., Cesare, B., Rubatto, D., London, D., and Morgan, G.B. VI (2010) Mechanisms of crustal anatexis: A geochemical study of partially melted metapelitic enclaves and host dacite, SE Spain. *Journal of Petrology*, 51, 785–821.
- Acosta-Vigil, A., London, D., and Morgan, G.B. VI (2012a) Chemical diffusion of major and minor components in granitic liquids: implications for the rates of homogenization of crustal melts. *Lithos*, 153, 308–323.
- Acosta-Vigil, A., Buick, I., Cesare, B., London, D., and Morgan, G.B. VI (2012b) The extent of equilibration between melt and residuum during regional anatexis and its implications for differentiation of the continental crust: A study of partially melted metapelitic enclaves. *Journal of Petrology*, 53, 1319–1356.
- Brown, J.A., Martins, T., and Černý, P. (2017) The Tanco Pegmatite at Bernic Lake, Manitoba. XVII. Mineralogy and geochemistry of alkali feldspars. *Canadian Mineralogist*, 55, 483–500.
- Burnham, C.W. (1979) Magmas and hydrothermal fluids. In H.L. Barnes, Ed., *Geochemistry of Hydrothermal Ore Deposits*, 2nd ed., 71–136. Wiley.
- Cameron, E.N., Jahns, R.H., McNair, A.H., and Page, L.R. (1949) Internal structure of granitic pegmatites. *Economic Geology Monograph*, 2, 115 p.
- Canosa, F., Martin-Izard, A., and Fuertes-Fuente, M. (2012) Evolved granitic systems as a source of rare element deposits; the Ponte Segade case (Galicia, NW Spain). *Lithos*, 153, 165–176.
- Carron, J.-P., and Lagache, M. (1980) Étude expérimentale du fractionnement des éléments Rb, Cs, Sr, et Ba entre feldspaths alcalins, solutions hydrothermales et liquides silicatés dans le système Q.Ab.Or.H₂O à 2 kbar entere 700 et 800°. *Bulletin de Minéralogie*, 103, 571–578.
- Černý, P. (1991) Rare-element granite pegmatites. Part I: anatomy and internal evolution of pegmatite deposits. *Geoscience Canada*, 18, 49–67.
- (1994) Evolution of feldspars in granitic pegmatites. In I. Parsons, Ed., *Feldspars and their reactions*. NATO Advanced Study Institutes Series C, *Mathematical and Physical Sciences*, 421, 501–540.
- (2005) The Tanco rare-element pegmatite deposit, Manitoba: regional context, internal anatomy, and global comparisons. In R.L. Linnen and I.M. Samson, Eds., *Rare-Element Geochemistry and Mineral Deposits*. Geological Association of Canada Short Course Notes 17, 127–158.
- Černý, P., and Chapman, R. (1984) Paragenesis, chemistry and structural state of adularia from granitic pegmatites. *Bulletin de Minéralogie*, 107, 369–384.
- Černý, P., Meintzer, R.E., and Anderson, A.J. (1985) Extreme fractionation in rare-element granitic pegmatites: selected examples of data and mechanisms. *Canadian Mineralogist*, 23, 381–421.
- Černý, P., London, D., and Novak, M. (2012) Granitic pegmatites as reflections of their sources. *Elements*, 8, 289–261.
- Chappell, B.W., and White, A.J.R. (2001) Two contrasting granite types: 25 years later. *Australian Journal of Earth Sciences*, 48, 489–499.
- Evensen, J.M., and London, D. (2003) Experimental partitioning of Be and other trace elements between cordierite and silicic melt, and the chemical signature of S-type granite. *Contributions to Mineralogy and Petrology*, 144, 739–757.
- Gordiyenko, V.V. (1971) Concentrations of Li, Rb, and Cs in potash feldspar and muscovite as criteria for assessing the rare-metal mineralization in granite pegmatites. *International Geology Review*, 13, 134–142.
- Heinrich, E.W. (1953) Zoning in pegmatite districts. *American Mineralogist*, 38, 68–87.
- Hulsbosch, N., Hertogen, J., Dewaele, S., André, L., and Muchez, P. (2014) Alkali metal and rare earth element evolution of rock-forming minerals from the Gatumba area pegmatites (Rwanda): Quantitative assessment of crystal-melt fractionation in the regional zonation of pegmatite groups. *Geochimica et Cosmochimica Acta*, 132, 349–374.
- Icenhower, J.P., and London, D. (1996) Experimental partitioning of Rb, Cs, Sr, and Ba between alkali feldspars and peraluminous melt. *American Mineralogist*, 81, 719–734.
- Ildefonse, J.P., Jambon, A., Carron, J.P., Delbove, F., and Gabis, V. (1979) La diffusion chimique dans les solutions hydrothermales et dans les verres et magmas silicatés. *Sciences Géologiques, Mémoire*, 53, 81–85.
- Jahns, R.H. (1953a) The genesis of pegmatites. I. Occurrence and origin of giant crystals. *American Mineralogist*, 38, 563–598.
- (1953b) The genesis of pegmatites. II. Quantitative analysis of lithium bearing pegmatite, Mora County, New Mexico. *American Mineralogist*, 38, 1078–1112.
- (1955) The study of pegmatites. *Economic Geology, Fiftieth Anniversary Volume: 1905–1955*, 1025–1130.
- (1982) Internal evolution of pegmatite bodies. In P. Černý, Ed., *Granitic Pegmatites in Science and Industry*, 8, p. 293–327. Mineralogical Association of Canada, Ottawa.
- Jahns, R.H., and Burnham, C.W. (1969) Experimental studies of pegmatite genesis: I. A model for the derivation and crystallization of granitic pegmatites. *Economic Geology*, 64, 843–864.
- Kontak, D.J., and Martin, R.F. (1997) Alkali feldspar in the peraluminous South Mountain Batholith, Nova Scotia: Trace-element data. *Canadian Mineralogist*, 35, 959–977.
- London, D. (2005) Geochemistry of alkali and alkaline earth elements in ore-forming granites, pegmatites, and rhyolites. In R.L. Linnen and I.M. Samson, Eds., *Rare-Element Geochemistry of Ore Deposits*, 17, p. 17–43. Geological Association of Canada Short Course Handbook.
- (2008) Pegmatites. *Canadian Mineralogist Special Publication*, 10, 368 p.
- (2014) A petrologic assessment of internal zonation in granitic pegmatites. *Lithos*, 184–187, 74–104.
- (2016) Rare-element granitic pegmatites. In P.L. Verplanck and M.W. Hitzman, Eds., *Rare Earth and Critical Elements in Major Deposit Types*, 18, p. 165–193. *Reviews in Economic Geology*.
- (2018) Ore-forming processes within granitic pegmatites. *Ore Geology Reviews*, 101, 349–383.
- London, D., and Morgan, G.B. VI (2012) The pegmatite puzzle. *Elements*, 8, 263–268.
- London, D., Hervig, R.L., and Morgan, G.B. VI (1988) Melt-aqueous solution solubilities and element partitioning in peraluminous granite-pegmatite systems: Experimental results with Macusani glass at 200 MPa. *Contributions to Mineralogy and Petrology*, 99, 360–373.
- London, D., Černý, P., Loomis, J.L., and Pan, J.J. (1990) Phosphorus in alkali feldspars of rare-element granitic pegmatites. *Canadian Mineralogist*, 28, 771–786.
- London, D., Morgan, G.B. VI, and Icenhower, J. (1998) Stability and solubility of pollucite in granitic systems at 200 MPa H₂O. *Canadian Mineralogist*, 36, 497–510.
- London, D., Hunt, L.E., Schwing, C.R., and Guttery, B.M. (2020a) Feldspar thermometry in pegmatites: truth and consequences. *Contributions to Mineralogy and Petrology*, 175. <https://doi.org/10.1007/s00410-019-1617-z>.
- London, D., Hunt, L.E., and Duval, C.L. (2020b) Temperatures and duration of crystallization in gem-bearing granitic pegmatites. *Lithos*, 360–361, 105417. <https://doi.org/10.1016/j.lithos.2020.105417>.
- London, D., Morgan, G.B. VI, Paul, K.A., and Guttery, B.M. (2012) Internal evolution of a miarolitic granitic pegmatite: The Little Three Mine, Ramona, California (U.S.A.). *Canadian Mineralogist*, 50, 1025–1054.
- Macdonald, R., Smith, R.L., and Thomas, J.E. (1992) Chemistry of the subalkalic silicic obsidians. U.S. Geological Survey Professional Paper, 214, 1523 p.
- Marchal, K., Simmons, W.B., Falster, A.U., Webber, K.L., and Roda-Robles, E. (2014) Geochemistry, mineralogy, and evolution of Li-Al micas and feldspars from the Mount Mica pegmatite, Maine, U.S.A. *Canadian Mineralogist*, 52, 221–233.
- Morgan, G.B. VI, and London, D. (1987) Alteration of amphibolitic wallrocks around the Tanco rare-element pegmatite, Bernic Lake, Manitoba. *American Mineralogist*, 72, 1097–1121.
- (1989) Experimental reactions of amphibolite with boron-bearing aqueous fluids at 200 MPa: Implications for tourmaline stability and partial melting in mafic rocks. *Contributions to Mineralogy and Petrology*, 102, 281–297.
- (1999) Crystallization of the Little Three layered pegmatite-aplite dike, Ramona District, California. *Contributions to Mineralogy and Petrology*, 136, 310–330.
- (2005) Phosphorus distribution between potassic alkali feldspar and metaluminous haplogranite liquid at 200 MPa (H₂O): The effect of undercooling on crystal-liquid systematics. *Contributions to Mineralogy and Petrology*, 150, 456–471.
- Mungall, J.E. (2002) Empirical models relating viscosity and tracer diffusion in magmatic silicate melts. *Geochimica et Cosmochimica Acta*, 66, 125–143.
- Nash, W.P., and Crecraft, H.R. (1985) Partition coefficients for trace elements in silicic magmas. *Geochimica et Cosmochimica Acta*, 49, 2309–2322.
- Neiva, A.M.R. (2014) Micas, feldspars and columbite-tantalite minerals from the zoned granitic lepidolite-subtype pegmatite at Namivo, Alto Ligonha, Mozambique. *European Journal of Mineralogy*, 25, 967–985.
- Neves, L.J.P.F., and Godinho, M.M. (1999) Structural state of K-feldspar in some Hercynian granites from Iberia; a review of data and controlling factors. *Canadian Mineralogist*, 37, 691–700.
- Parsons, I., Magee, C.W., Allen, C.M., Shelley, J.M.G., and Lee, M.R. (2009) Mutual replacement reactions in alkali feldspars II: trace element partitioning and geothermometry. *Contributions to Mineralogy and Petrology*, 157, 663–687.
- Ren, M. (2004) Partitioning of Sr, Ba, Rb, Y, and LREE between alkali feldspar and peraluminous silicic magma. *American Mineralogist*, 89, 1290–1303.
- Roda-Robles, E., Pesquera, A., Gil-Crespo, P., and Torres-Ruiz, J. (2012) From granite to highly evolved pegmatite: a case study of the Pinilla de Femoselle granite-pegmatite system (Zamora, Spain.). *Lithos*, 153, 192–207.

- Roselieb, K., and Jambon, A. (1997) Tracer diffusion of potassium, rubidium, and cesium in a supercooled jadeite melt. *Geochimica et Cosmochimica Acta*, 61, 3101–3110.
- Roy, B.N., and Navrotsky, A. (1984) Thermochemistry of charge-coupled substitutions in silicate glasses: The systems $M_{in}^{+}AlO_2-SiO_2$ ($M = Li, Na, K, Rb, Cs, Mg, Ca, Sr, Ba, Pb$). *Journal of the American Ceramic Society*, 67, 606–610.
- Royzman, F.N. (1982) Geochemical features and exploration value of various genetic types of biotite metasomatites in a rare-metal pegmatite field. *International Geology Review*, 24, 24–30. doi: 10.1080/00206818209452363.
- Saasen, A., Jordal, O.H., Burkhead, D., Berg, P.C., Løklingholm, G., Pedersen, E.S., Turner, J., and Harris, M.J. (2002) Drilling HT/HP wells using a cesium formate based drilling fluid. Society of Petroleum Engineers, document SPE-74541-MS, <https://doi.org/10.2118/74541-MS>.
- Shannon, R.D. (1976) Systematic studies of interatomic distances in oxides. In R.G.J. Strens, Ed., *The Physics and Chemistry of Minerals and Rocks*, p. 403–431. Wiley.
- Shearer, C.K., Papike, J.J., and Jolliff, B.L. (1992) Petrogenetic links among granites and pegmatites in the Harney Peak rare-element granite-pegmatite system, Black Hills, South Dakota. *Canadian Mineralogist*, 30, 785–809.
- Smith, V.G., Tiller, T.P., and Rutter, J.W. (1955) A mathematical analysis of solute redistribution during solidification. *Canadian Journal of Physics*, 33, 723–744.
- Stilling, A., Černý, P., and Vanstone, P.J. (2006) The Tanco pegmatite at Bernic Lake, Manitoba. XVI. Zonal and bulk compositions and their petrogenetic significance. *Canadian Mineralogist*, 44, 599–623.
- Teertstra, D.K., Černý, P., and Hawthorne, F.C. (1999) Geochemistry and petrology of late K- and Rb- feldspars in the Rubellite pegmatite, Lilypad Lakes, NW Ontario. *Canadian Mineralogist*, 65, 237–247.
- Volfinger, M. (1969) Partage de Rb et Cs entre sanidine, muscovite et solution a 600°C, 1,000 bars. *Comptes Rendus Hebdomadaires Des Seances de L'Academie Des Sciences, Serie D: Sciences Naturelles*, 269, 1–3.
- Webster, J.D., Holloway, J.R., and Hervig, R.L. (1989) Partitioning of lithophile trace elements between H_2O and $H_2O + CO_2$ fluids and topaz rhyolite melt. *Economic Geology*, 84, 116–134.

MANUSCRIPT RECEIVED OCTOBER 14, 2020

MANUSCRIPT ACCEPTED JANUARY 6, 2021

MANUSCRIPT HANDLED BY CALVIN G. BARNES

Endnotes:

¹Deposit item AM-22-17855, Online Materials. Deposit items are free to all readers and found on the MSA website, via the specific issue's Table of Contents (go to http://www.minsocam.org/MSA/AmMin/TOC/2022/Jan2022_data/Jan2022_data.html).

² Jahns and Burnham (1969) regarded the converse as true: the typical plutonic texture of granite arises from the crystallization of the melt alone in the absence of an aqueous solution. Burnham (1979) proposed a model for the generation of subduction-related base-metal deposits in which an aqueous solution separated early in the crystallization of a granitic magma body, but quartz veins, not pegmatite dikes, were generated in the process. The contradiction between this model and that of Jahns and Burnham (1969) has not been addressed. Černý et al. (2012) observed that pegmatites are absent from these subduction-related base-metal granitoids unless they contained an added fluxing component, such as boron, from marine sediment or altered oceanic crust.